Arab J Sci Eng (2017) 42:375–381
DOI 10.1007/s13369-016-2050-5

RESEARCH ARTICLE - PHYSICS

Analysis Techniques for Photovoltaic Modules Based on Amorphous Solar Cells

K. Agroui[1] · **M. Pellegrino**[2] · **F. Giovanni**[2]

Received: 17 January 2015 / Accepted: 20 January 2016 / Published online: 8 February 2016

Abstract This paper focuses on the description of the analysis techniques of the PV module based on amorphous solar cells under indoor aging tests according to IEC 61646. The goal of this work is the knowledge about the dynamic characteristics of the PV module. The effect of indoor aging on the PV module performances will be also described. For this purpose, a simple technique, based on the analysis of the behavior of PV module biased by an AC signal on dark conditions, has been described and experimented. This technique allows evaluating easily and quickly some parameters such as the series, the parallel resistances and the capacitance affecting the dynamic AC model of the PV module.

Keywords Photovoltaic module · Thin solar films · Indoor aging · Electrical performances · Impedance spectroscopy

List of symbols

I_{SC}	Short circuit current (V)
V_{OC}	Open circuit voltage (V)
η_c	Efficiency of solar cell (%)
η_m	Efficiency of PV module (%)
FF	Fill factor (%)
P_{max}	Maximum power (W)
V_{mp}	Current at maximum power point (V)
V_{mp}	Voltage at maximum power point (V)
R_s	Serial resistance (Ω)
R_{sh}	Shunt resistance (Ω)

✉ K. Agroui
kagroui@yahoo.fr

[1] Semiconductors Technology for Energetic Research Center(CRTSE), 2, Bd. Dr. Frantz Fanon, BP 140 Alger 7 Merveilles, Algiers, Algeria

[2] Italian National Agency for New Technologies (ENEA), Area Granatello, Portici, 80055 Naples, Italy

1 Introduction

More than 90 % of photovoltaic (PV) solar modules produced, for terrestrial applications, are made from crystalline silicon solar cells. However, in the past 2 years, thin films solar modules based on amorphous silicon (a-Si), cadmium telluride (CdTe), copper indium selenide (CIS) and gallium arsenide (GaAs) have gained a strong foothold in the world PV market and PV modules thin film technology becomes one of the most promising PV branches modules. The Advantages of thin films technology are [1]:

- Savings in material and energy consumption;
- Half number of process steps;
- Large area deposition;
- Implementation in building industry.

The stability of peak power of thin films PV modules after long-term outdoor exposure is a crucial parameter for the reliability and durability. In real life, however, all degradation mechanisms influence the life of a PV module. Accelerated aging methods are employed for qualification in defined testing sequences. The test sequence of thin films PV modules for the design qualification and type approval as described in IEC 61646 have become a pass/fail indicator whether the product is qualified for sale. However, qualification testing is not a method for a quantitative prediction of the products service life in general [2]. Accelerated aging tests, such as damp heat, humidity freeze and UV irradiation, combined with mechanical stress and other factors, such as corrosive atmosphere, add to degradation and in combination with each other form a complex array of interacting factors.

A number of analytical and characterization methods are conventionally employed to measure and determine the PV

module performances and components degradation like thin conductive materials. For example, current–voltage (I–V), quantum efficiency (QE), photoluminescence (PL) and electroluminescence (EL) measurements are used to allow a direct evaluation of the quality of the solar cells or PV modules [3]. These methods are in general complementary.

In the framework of a larger PV modules testing program, aimed at studying the degradation phenomena induced by stressing environmental conditions, ENEA is developing a simple technique based on the behavior of the PV devices, when they are biased by an AC signal on the dark spectroscopy impedance (IS) analysis. This technique is based on the consideration that for PV module based on different solar cell technologies, EVA encapsulant will decompose to produce acetic acid, lowering the pH and increasing the surface corrosion rates of embedded devices [4,5]. The acetic acid resulting from EVA degradation (deacetylation reaction) can at the same time accelerate the oxidation of the metallic conductors and causing an increase in the ohmic resistance. Therefore, EVA deterioration leads to a decrease in the shunt resistance and affects the properties of other solar cell components.

In comparison, IS technique is well known to be highly suitable for analyzing a variety of R–C circuits corresponding to a large number of physical materials and devices [6]. Specifically, IS measurements can readily allow a quantitative evaluation of the electrical property of a solar cell's PN junction, which is typically represented by an equivalent circuit of a parallel resistor and capacitor (R–C circuit model) and its series resistance.

Briefly, in a simplest form of the IS measurements, a small amplitude sinusoidal AC signal is applied to the PV module over a range of frequency. The PV module responses can be identified by mapping the real and imaginary parts of their complex impedance as a function of the frequency of the applied external electric field as shown in Fig. 1.

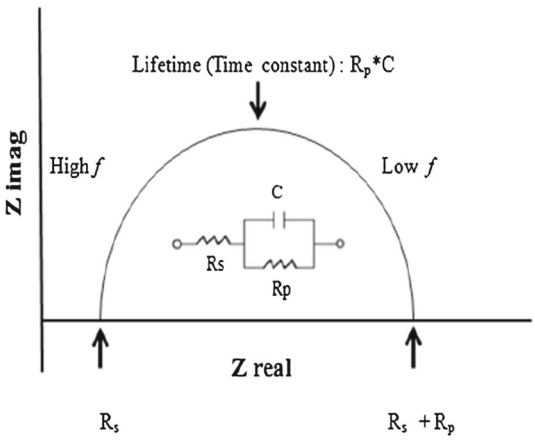

Fig. 1 General Nyquist plot for PV solar cell

The main purpose of this research work is to investigate the performances recovery of the amorphous PV module during the qualification indoor testing. The possibility to introduce the IS measurements to more understand and quantify any relevant PV modules performances change, as a complementary non-destructive analysis, will be examined. The frequency- and voltage-dependent characteristics of PV module are determined by IS technique and frequency response analysis, based on sinusoidal and periodic signals.

2 Experimental

2.1 PV Module Description

The tested PV module type NH 100 AX from NEX POWER manufacturer is based on a-Si:H solar cells. The area of each solar cell is 118 cm^2. The module size (LxW) is 1.42 m × 1.19 m. Solar cells are arranged in 119 series connected cells using glass–glass configuration. The maximum power of the PV module was rated at 90W, but the power, in anticipation of power loss due to the Staebler–Wronski effect, was estimated by its manufacturer to produce 15 % more than its rated power when first deployed.

2.2 Indoor Aging Conditions

2.2.1 Salt Spray Test

The salt spray test is executed by using a corrosion chamber according to IEC 61701 [7]. The chamber can operate in a temperature range between room temperature and 55 °C and on the relative humidity range between 50 % and over the saturation condition (rain). The pre-prepared mixture of water within concentration salinity of 5 % and acetic acid solution within pH = 3.7 is sprayed upright, where PV module is held on a special rack at a fixed slope of 20° with respect to the vertical line. The test duration is 96 h where the PV module is sprayed for 5 min at each hour.

2.2.2 Humidity Freeze Test

The purpose of this test is to determine the withstand ability of the PV module to laminate, which is consisting of different materials with varying thermal expansion coefficient, against humidity penetration under the effects of high temperature and humidity followed by sub-zero temperatures. PV module is subjected to cycling between temperatures 85 °C with relative humidity 85 % and −40 °C. The humidity freeze (HUF) test is realized in the climatic chamber type PV 8500 from Angelantoni Industrie SpA (Italy) according to test 10.12 of IEC 61646 [8]. PV module is then subjected to 10 complete HUF cycles in the closed climatic chamber.

2.2.3 UV Test

The qualification tests such as described in IEC 61646 include a UV preconditioning test. This test is often used for evaluating the UV stability of PV packaging materials, which is necessary to evaluate PV module reliability [9]. The UV test is realized in thermal chamber type UV 3000 from Angelantoni Industries SpA (Italy). The goal of this test is to accelerate the photodegradation processes occurring in the EVA encapsulant material. These processes include chain scission, for example due to long exposure UV radiations especially UVA and UVB part of the spectrum [10]. PV module has been aged under UV conditions with humidity at 20 % (dry conditions) at temperature of 60 °C. Artificial light source-type metal halide arc lamps has been used for indoor exposure UV. The UV irradiation intensity during the test in the wavelength range from 280–385 and 280–320 nm, is 15 and 5 kWh/m^2, respectively. Lamp spectrum measurements were carried out using a spectroradiometer type SR, 9910 V7 from Macam Photometrics Ltd (Scotland). The lamp intensity was recorded as a function of wavelength in the range 200–800 nm with a step wavelength of 1 nm and the scan time of 100 ms per step. Figure 2 shows the measured spectral distribution of the UV lamp intensity. The lamp intensity spectrum contains 250 and 15 W/m^2 in the wavelength range from 280–385 and 280–320 nm, respectively. The values of the lamp intensity seem very high. For comparison, the AM 1.5 solar spectrum contains 35.3 and 1.52 W/m^2 in the wavelength range from 280–385 and 280–320 nm, respectively.

2.3 Analysis Techniques

2.3.1 I–V under Illumination Measurements

Variations in the I–V characteristics due to indoor aging can lead to power losses in PV module. This test is carried out with a solar simulator type Pasan Sun Simulator class IIIA according to IEC-60904-9 which determines the electrical parameters under standard test conditions (STC -irradiance: 1000 W/m^2, AM 1.5 spectrum; module temperature: 25 °C). In order to thoroughly analyze the module degradation process, a simple degradation factor has been used. This degradation factor (D_f) is computed using the relation (1):

$$D_f = \frac{P_{m,f} - P_{m,i}}{P_{m,i}} \quad (1)$$

where:

$P_{m,i}$: maximum power at STC conditions before degradation

$P_{m,f}$: maximum power at STC conditions after degradation

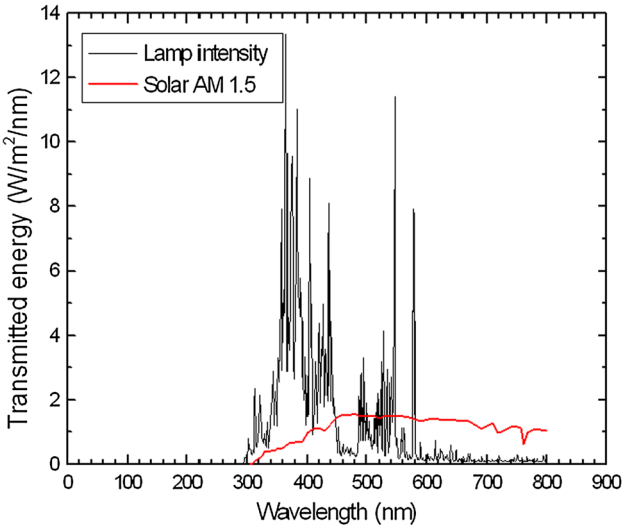

Fig. 2 Variation in UV lamp intensity as function of wavelength

2.3.2 Capacitive and Complex Impedance Analysis

During AC measurement, a small sinusoidal signal of 50 mV peak to peak is superimposed over the DC bias voltage set at 0 V, with frequency ranging from less than 1 Hz to about 1 MHz. The measurements for the capacitive and complex impedance analysis were carried out using impedance analyzer Solartron 1260, dielectric interface Solartron 1296, impedance analyzer Hewlett-Packard 4192 A. The PV module is kept in a controlled climatic chamber type Perani CT 700 for all IS measurements in order to avoid any thermal effect.

3 Results and Discussions

3.1 Indoor PV Module Degradation Analysis

Figure 3 shows the I–V characteristics of the PV module type NH 100 AX, based on single amorphous solar cells, before and after indoor aging tests.

The PV module exhibited an increase in the maximum power (P_{max}) and no noticeable changes in the open circuit voltage (V_{oc}) and the short current circuit (I_{sc}) under STC conditions. After indoor aging like salt spray corrosion, UV radiation and humidity freeze, the P_{max} has increased by 0.52, 7.86 and 13.0 %, respectively. Table 1 shows the PV module performances under indoor aging tests.

Fill factor (FF) was proposed to describe the PV module performance due to its sensitivity to the resistance characteristics of the PV module and environment parameters. The ground state of the a-Si PV module was 60.51 % in fill factor, while an increase in FF finally leaded to a saturated state around 63.90 and 66.36 % after UV and humidity freeze

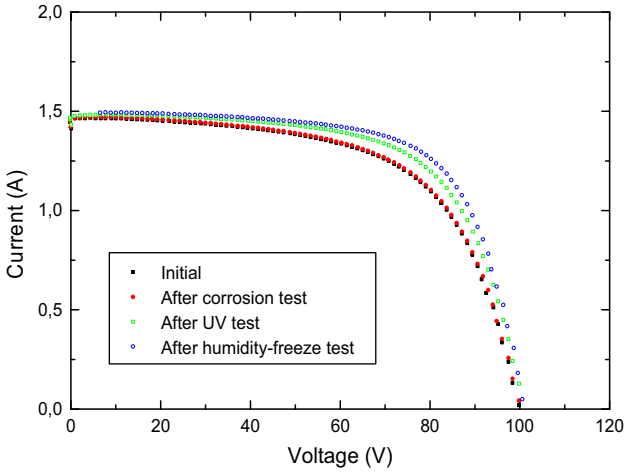

Fig. 3 Current versus voltage characteristic for the PV module type NH 100 AX at STC conditions for different aging tests

Table 1 PV module type NH 100 AX performances at STC conditions for different aging tests

	Initial	Corrosion	UV	Humidity freeze
I_{SC} (A)	1.48	1.48	1.50	1.50
V_{OC} (V)	99.74	100.24	100.9	101.24
η_c (%)	6.29	6.32	6.8	7.1
η_m (%)	5.70	5.73	6.10	6.40
FF (%)	60.46	60.43	63.90	66.36
P_{max} (W)	89.65	90.12	96.71	101.28
V_{mp} (V)	75.88	75.88	77.1	79.39
I_{mp} (A)	1.18	1.18	1.26	1.276
R_S (Ω)	10.74	11.3	9.6	8.888
R_{sh} (Ω)	639.30	654.70	911.29	1047.50

test, respectively. Obviously, it is suggested that the recovery behavior occurs when heating up the a-Si PV module, and the performance itself is influenced by annealing parameters.

According to the literature review, the annealing behavior of a-Si PV module is a complex phenomenon, with two kinetic components employing fast and slow metastable defects in a-Si solar cell [11]. In fact, the annealing recovery behavior is attributed to the diffusion of atoms and the diffusion kinetics is dominantly determined by the temperature [12]. Thus, it is suggested that a slow recovery mechanism behavior is revealed due to a slow annealing temperature, when heating up the PV module during qualifications tests. Accordingly, recovery mechanism should occur and results in a better performance of the solar cell [13]. The recovery behavior is due to the elimination of metastable defects and may also help to reduce the electrical resistance within solar cell [14]. In the current study, apparently, the decrease in R_s in a-Si module should be attributed to the recovery behavior. Thus, these metastable effects do not contradict the long-term stability of amorphous PV module.

It is revealed that a recovery behavior of a-Si was observed at low temperature (below 85 °C), after UV and humidity freeze indoor test. FF values in a-Si increase, while R_s was reversely decreased. Thus, it can be deduced that a recovery was mainly governed by temperature. The increase in FF in a-Si when raising the PV module temperature should be due to the decrease in R_s.

Visual inspection was performed revealing that physical changes were imperceptible due to the stability of EVA additives during indoor aging tests [15]. The results show that P_{max} gain is below 15 % due to Staebler–Wronski effect.

The effects of indoor aging tests on amorphous PV module performance without preliminary stabilization tests have been observed. Characterizing the performance of a-Si PV module is found to be a non-trivial task, due to the variations caused by time-dependent and reversible effects [16,17]. The PV module performance improves during the indoor aging tests due to the accumulated effects of higher module operating temperature and light exposure. When the relative change in power of the PV module was higher than the nominal previous measured value, then the module was considered as in a non-stabilized state. For this reason, amorphous thin films PV modules are submitted to light soaking [18] and annealing [19] according to IEC 61646. These tests are executed before any indoor thermal tests, in order to separate the annealing effects from any degradation resulting from these tests, until P_{max} is stable within 2 %.

The PV module insulation test was also investigated. The purpose of the insulation test is to determine whether or not the PV module is sufficiently well insulated between current carrying parts and the frame. The apparatus used is Sefelec MPC47P. The insulation test results show that the PV module exhibits no dielectric breakdown or surface tracking during each aging step. Furthermore, the measured insulation resistance of the module at ambient temperature and in a relative humidity not exceeding 75 % was not less than 40 MΩ · m^2 according to IEC 61646 code 10.3 [20]

3.2 Dynamic Measurements in AC Mode

3.2.1 Capacitance Measurements as Function of Voltage and Frequency

Complementary PV module information was obtained from the AC signal. In the dark frequency response analysis, the PV module is electrically connected to an AC supplier at room temperature. Useful information on the quality of the PV module can be derived from their different analysis curves. Figure 4 shows the variation in the capacitance versus voltage (C–V) from the forward and reverse C–V sweep modes in

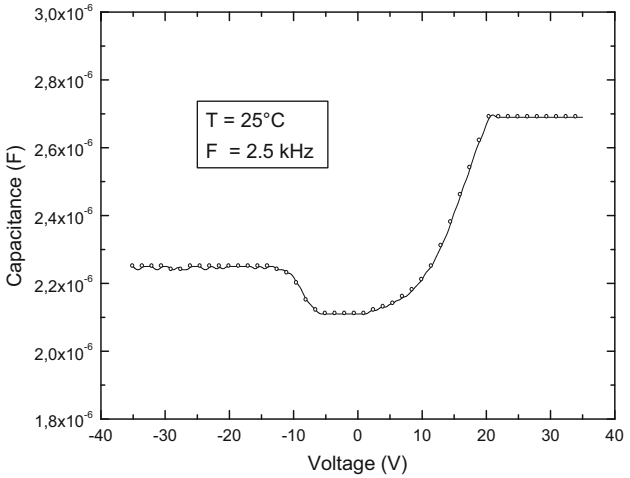

Fig. 4 Capacitance versus voltage characteristic for the PV module type NH 100 AX

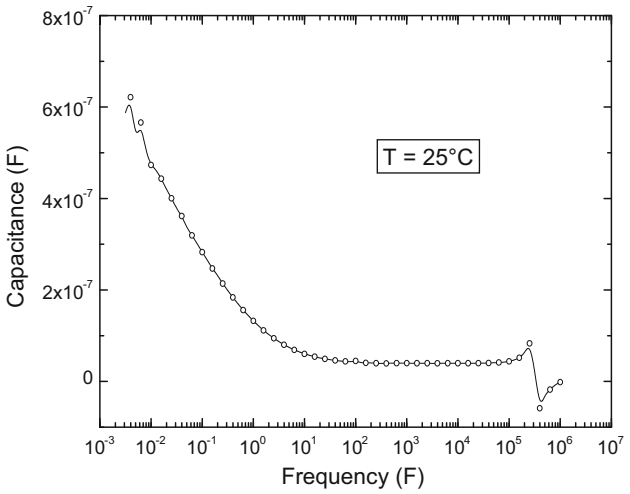

Fig. 5 Capacitance versus frequency for the PV module type NH 100 AX

the range of −35 to +35 V at a constant frequency of 2.5kHz and ambient temperature of 25 °C.

The experimental results show that capacitance varies with applied voltage. C–V analysis provides investigation about the complex behavior of the capacitance toward the voltage in reverse and forward bias. Different regions are detected where junction capacitance prevails in the reverse region and diffusive capacitance at forward bias, where the average life time of the charge carriers is related. The C–V has three regimes of accumulation, depletion and inversion regions [21]. It is noted that the capacitance increases for bias voltage higher than 0 V and stabilizes for potential values higher than 20 V.

Figure 5 shows the variation in the capacitance versus frequency (C–f) in the range of 10^{-3}−10^{6}Hz at ambient temperature of 25 °C.

The physical meaning of the capacitance is not at all clear; in fact, it should be related to the quality of the PN junction, depending on the particular region of the frequency and on the bias voltage at which the value is determined. The experimental results show that capacitance varies with applied voltage frequency. For frequency high values (100 kHz), the capacitance can be assumed to be the geometric capacitance of the junction, whereas at frequency low values (10^{-3} Hz) it is affected by the presence of defects density in the a-Si bulk. That could explain the increase in the capacitance at frequency low values. This effect is explained in the literature, for a true capacitance, as due to the increasing of the dielectric constant as soon as the frequency is lowering. There is an intermediate region where the capacitance is almost independent on the frequency; it is considered to be the geometrical capacitance, and its value is used to give an estimation of the depletion layer thickness. The range of the frequency where this happens is in the range of 10 HZ–100 kHz. But even if the PV module presents capacitive effects, they are not real capacitance and the increasing of capacitance values at very low frequencies has also been related to signals deriving from imperfections, flaws and defects within the material [22]. For a-Si PV module, it could be the defects state density or the presence of traps; their signals at high frequency cannot be revealed because they cannot follow the rapid change in the voltage, but at higher temperature or at lower frequency they are allowed to appear. The difference between the low frequency stabilized capacitance value and the geometrical value has been referred as the extra-capacitance; since the amorphous modules do not reach the stabilized value at the frequency of measurement and it becomes difficult to make the measurement below 1 Hz due to the presence of the background noise, their extra-capacitance values are not very accurate.

3.2.2 Impedance Spectroscopy Measurements

Figure 6 shows the complex impedance of the PV module type NH 100 AX at the constant temperature of 25 °C. The real and imaginary parts of the complex impedance are shown in Fig. 6a, b, respectively.

Imaginary part of the complex impedance (Z_{imag}) reaches positive values at highest frequencies. While Z_{imag} is negative, the sample has a capacitive character. From these curves, the equivalent circuit model of the PV module type NH 100 AX can be derived. At frequency of 3.10^{-3} Hz (low frequency), the real part of the complex impedance (Z_{real}) is 1 MΩ. At frequency of 1 MHz (high frequency), Z_{real} is 270Ω. From these results, the resistors R_s and R_p of the equivalent AC circuit model are calculated to be 270 Ω and 1MΩ, respectively. The capacitance C_p is calculated to be 53μF. This result is derived from the measured Z_{imag} impedance of the photovoltaic module. We therefore arrive

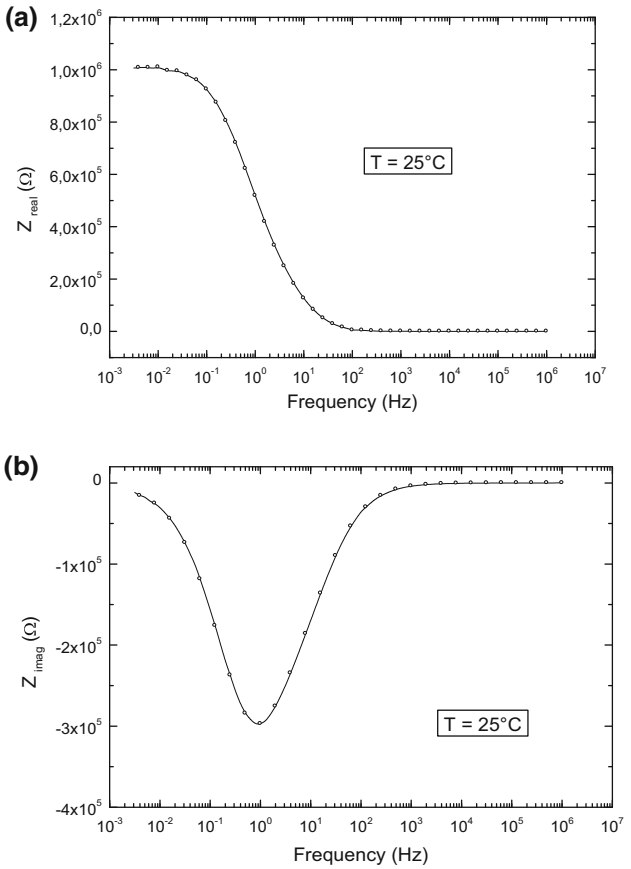

Fig. 6 Complex impedance of the PV module type NH 100 AX. **a** Real impedance (Z_{real}). **b** Imaginary impedance (Z_{image})

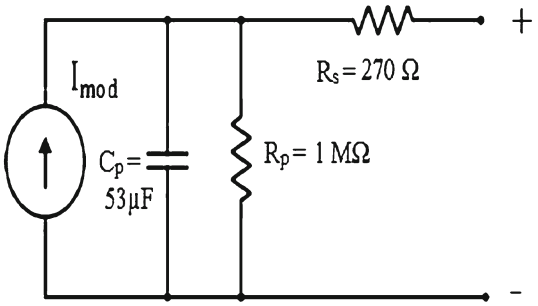

Fig. 7 Dynamic equivalent circuit model of the PV module type NH 100 AX

at the following simplified equivalent AC circuit model of the measured PV module as shown in Fig. 7.

The Nyquist plot is obtained by applying the IS technique to the PV module as shown in Fig. 8. In this case, the expected shape of the Nyquist plot has been found [23]. The only difference is that for the single solar cell the Nyquist curve is precisely a semi-circumference, while for the PV module, assumed as an electrical connection of a lot of cells within mismatch factor dispersion, the curve is much more like an ellipse with 11.1 % of eccentricity. That means, in case of the

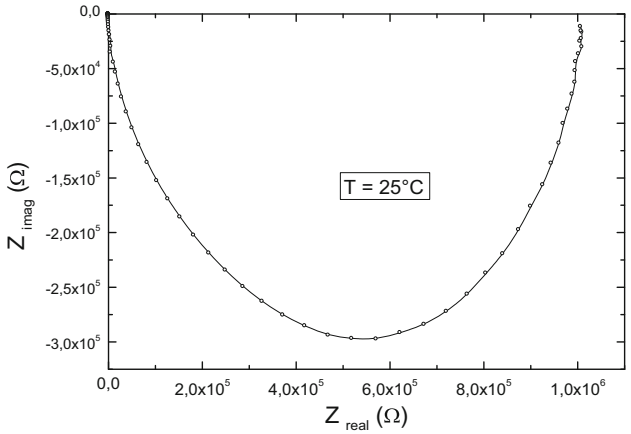

Fig. 8 Nyquist impedance plot for the PV module type NH 100 AX

PV module there is an inductance effect, probably due to the closed circuitry.

4 Conclusion

Two different experiments were conducted to gain information on the behavior of PV module based on amorphous solar cells. Firstly, a major phenomenon related to instability of metastable behavioral that affect indoor PV module performance is described. Contrarily to crystalline PV modules, amorphous PV modules require more stabilization by light soaking and thermal annealing before any qualification test procedure. Secondly, we have demonstrated the interest of IS as a sensitive and non-destructive analytical technique as well as its highly complementary capability to conventional analysis techniques in the characterization of PV module performance and reliability. Accordingly, the dynamic characterizations provide adequate information for the PV module as a good diagnostic technique to monitor PV module degradation process.

Acknowledgments The authors would like to express their gratefulness to Dr C. Privato from ENEA Portici for his valuable collaboration and technical assistance.

References

1. Agroui, K.; Hadj Mahammed, I.; Hadj Arab, A.; Belghachi, A.: Characterization photovoltaic modules based on thin films solar cells in environmental operating conditions of Algerian Sahara. Proc. SPIE **7048**, 1–8 (2008)
2. Wohlgemuth, J.; Kempe, M.; Miller, D.; Kurtz, S.: Developing standards for PV packaging materials. Proc. SPIE **8112**, 1–8 (2011)
3. Schlothauer, J.; Jungwirtha, S.; Kohl, M.; Order, B.: Degradation of the encapsulant polymer in outdoor weathered photovoltaic modules: Spatially resolved inspection of EVA ageing by fluorescence

and correlation to electroluminescence. Sol. Energy Mater. Solar Cells **102**, 75–85 (2012)
4. Pern, F.J.; Czanderna, A.W.: Characterization of ethylene vinyl acetate (EVA) encapsulant: Effects of thermal processing and weathering degradation on its discoloration. Sol. Energy Mater. Sol. Cells **25**, 3–23 (1992)
5. Agroui, K.; Collins, G.; Giovanni, F.; Stark, W.: A Comprehensive indoor and outdoor aging of the cross-linked EVA encapsulant material for photovoltaic conversion. Polym. Plast. Technol. Eng. **54**(7), 719–729 (2015)
6. Pern, F.J.; Noufi, R.: Characterization of damp-heat degradation of CuInGaSe2 Solar cell components and devices by (electrochemical) impedance spectroscopy. Proc. SPIE **8112**, 1–14 (2011)
7. Salt mist corrosion testing of photovoltaic (PV) modules. In: IEC 61701, Ed. 1995-03
8. Humidity freeze test sequence, code 10.12. In: IEC 61215, Ed. 1995-03
9. Kempe, M.D.: Accelerated UV test methods for encapsulant of photovoltaic modules. In: Proceedings of the 33rd IEEE Photovoltaic Specialist Conference, San Diego, California (USA), 11–16 May 2008
10. UV preconditioning test sequence, code 10.10. In IEC 61215, Ed. 1995-03
11. Yang, L.; Chen, L.: Fast and slow metastable defects in hydrogenated amorphous silicon. Appl. Phys. Lett. **63**, 400–402 (1993)
12. Shewmon, P.: Diffusion in Solids, The Minerals, Metals and Materials Society, 2nd edn. (1989)
13. Myong, S.Y.: Annealing kinetic model using fast and slow metastable defects for hydrogenated amorphous-silicon-based solar cells. Adv. Opto-Electron. **2007**, 1–8 (2007)
14. Hsieh, H.H.; Cheng, J.S.: Recovery behavior in amorphous silicon solar module at low temperature. In: 34th IEEE Photovoltaic Specialists Conference (PVSC), Philadelphia, PA, pp. 486–488 (2009)
15. Reid, Charles G.; Bokria, Jayesh G.; Woods, Joseph T.: UV aging and outdoor exposure correlation for EVA PV encapsulants. Proc. SPIE **8825**, 1–11 (2013)
16. Nikolaeva-Dimitrova, M.; Kenny, R.P.; Dunlop, E.D.: Long term stability of a-Si:H thin film modules. In: 21st European Photovoltaic Solar Energy Conference, Dresden, Germany, 4–8 September 2006
17. Nikolaeva-Dimitrova, M.; Kenny, Robert P.; Dunlop, Ewan D.: Controlled conditioning of a-Si:H thin film modules for efficiency prediction. Thin Solid Films **516**, 6902–6906 (2008)
18. Light soaking test sequence, code 10.18. In: IEC 61646, Ed. 1995-03
19. Annealing test sequence, code 10.19. In: IEC 61646, Ed. 1995-03
20. Dechthummarong, C.; Wiengmoon, B.; Chenvidhya, D.; Jivacate, C.; Kirtikara, K.: Physical deterioration of encapsulation and electrical insulation properties of PV modules after long-term operation in Thailand. Sol. Energy Mater. Sol. Cells **94**(9), 1437–1440 (2010)
21. Pellegrino, M.; Nardelli, G.; Sarno, A.: An Indoor technique for assessing the degradation of PV modules. 14th European Photovoltaic Solar Energy Conference, Barcelona (Spain), 30 June–4 July 1997
22. Pellegrino, M.; Flaminio, G.; Sarno, A.; Zhao, J.: Dark measurements technique for PV modules quality evaluation. In: 17th European Photovoltaic Solar Energy Conference, Munich (Germany), 22–26 October 2001
23. Chenvidhya, D.; Kirtikara, K.; Jivacate, C.: A new characterization method for solar cell dynamic impedance. Sol. Cells Sol. Energy Mater. Sol. Cells **80**, 459–464 (2003)